 CMES, vol.96, no.6, pp.435-455, 2013

SPH and ALE Formulations for Fluid Structure Coupling

R. Messahel[1] **and M. Souli**[1]

Abstract: Simulation of Fluid Structure Interaction FSI, problems becomes more and more the focus of computational engineering, where FEM (Finite element Methods) for structural mechanics and Finite Volume for CFD are dominant. New formulations have been developed for FSI applications using mesh free methods as SPH method, (Smooth Particle Hydrodynamic). Up to these days very little has been done to compare different methods and assess which one would be more suitable. For small deformation, FEM Lagrangian formulation can solve structure interface and material boundary accurately; the main limitation of the formulation is high mesh distortion for large deformation and moving structure. One of the commonly used approach to solve these problems is the ALE formulation which has been used with success in the simulation of fluid structure interaction with large structure motion such as sloshing fuel tank in automotive industry and bird impact in aeronautic industry. For some applications, including bird impact and high velocity impact problems, engineers have switched from ALE to SPH method to reduce CPU time and save memory allocation.
In this paper the mathematical and numerical implementation of the ALE and SPH formulations are described. From different simulation, it has been observed that for the SPH method to provide similar results as ALE or Lagrangian formulations, the SPH meshing, or SPH spacing particles needs to be finer than the ALE mesh. To validate the statement, we perform a simulation of a shock wave propagation generated by explosive detonation. For this simple problem, the particle spacing of SPH method needs to be at least two times finer than ALE mesh. A contact algorithm is performed at the fluid structure interface for both SPH and ALE formulations.

Keywords: ALE, SPH, Fluid Structure Interaction, Shock Wave.

1 Introduction

Theoretical and experimental analysis of underwater explosion have been considered by several researchers over the past decades, using empirical methods as CON-

[1] Université de Lille1, Laboratoire de Mécanique de Lille (LML), UMR CNRS 8107, FRANCE.

WEAP(Conventional Weapon) code when the explosive charge is far away from the structure, and Lagrangian description of motion for near field. In its formulation, CONWEAP code does not represent the physical behavior of detonation. When a high explosive is detonated an inward wave is generated in the explosive material, at the same time, a shock wave moves through the air medium, which is at lower pressure and a contact discontinuity appears between the rarefaction wave and the shock wave. Experiments have shown, see Kingery and Bulmarsh (1984), that the resulting flow is quite complex, involving several physical phenomena as burning effects and heat transfer. The detonation of high explosive material converts the explosive charge into gas at high pressure and temperature what leads to damage structures. Numerical simulation of high explosive detonation and expansion are very difficult for classical numerical methods, see Boyer (1960). During the process in the explosion, a very thin reaction zone divides the domain into inhomogeneous parts and produces large deformations. Numerical simulation using appropriate equation of state for high explosive detonation, helps to describe these phenomena, and also minimize the number of tests required that are very costly. Once simulations are validated by test results, it can be used as design tool for the improvement of the system structure involved. Initially FEM Lagrangian were used to simulate these problems, unfortunately classical Lagrangian methods cannot resolve large mesh distortion, runs are stopped befor reaching termination time, due to negative Jacobian in highly distorted element. ALE multi-material description of motion developed in Aquelet, Souli and Olovson (2005) can be used as an alternative for the simulation of high explosive phenomena. The ALE formulations have been developed to overcome the difficulties due to large mesh distortion. For some applications, including underwater explosions and their impact on the surronding structure, engineers have switched from ALE to SPH method to reduce CPU time and save memory allocation.

It is well known from previous papers, see Ozdemir, Souli and Fahjan (2010) that the classical FEM Lagrangian method is not suitable for most of the FSI problems due to high mesh distortion in the fluid domain. In many applications the ALE formulation has been the only alternative to solve fluid structure interaction for engineering problems. For the last decade, SPH method has been used usefully for engineering problems to simulate high velocity impact problems, high explosive detonation in soil, underwater explosion phenomena, and bird strike in aerospace industry. SPH is a mesh free Lagrangian description of motion that can provide many advantages in fluid mechanics and also for modeling large deformation in solid mechanics. Unlike ALE method, and because of the absence of the mesh, SPH method suffers from a lack of consistency than can lead to poor accuracy.

In this paper, devoted to ALE and SPH formulations for fluid structure interaction

problems, the mathematical and numerical implementation of the ALE and SPH formulations are described. From different simulation, it has been observed that for the SPH method to provide similar results as ALE formulation, the SPH meshing, or SPH spacing particles needs to be finer than the ALE mesh. To validate the statement,, we perform a simulation of a shock wave propagation generated by explosive detonation. For this problem, the particle spacing of SPH method needs to be at least two times finer than ALE mesh. A contact algorithm is performed at the fluid structure interface for both SPH and ALE formulations.

In Section 2, the governing equations of the ALE formulation are described. In this section, we discuss the advection algorithms used to solve mass, momentum and energy conservation in the multi-material formulation. Section 3 describes the SPH formulation, unlike ALE formulation which based of the Galerkin approach, SPH is a collocation method. The last section is devoted to numerical simulation of an underwater explosion and its impact on a deformable structure using both ALE and SPH methods. To get comparable between ALE and SPH, the particle spacing of SPH method needs to be at least two times finer than ALE mesh.

2 ALE Multi-material formulation

A brief description of the ALE formulation used in this paper is presented, additional details can be provided in Aquelet, Souli and Olovson (2005). To solve fluid structure interaction problems, a Lagrangian formulation is performed for the structure and an ALE formulation for the fluid and explosive materials, where fluid and explosive materials can be mixed in the same element, this element is referred as mixed element, since it contains two different materials fluid and explosive as described in Fig. 1. A mixture theory is used to partition the material inside the element and compute the volume weighted stress from the constitutive model of each material as described in Souli and Erchiqui (2011).

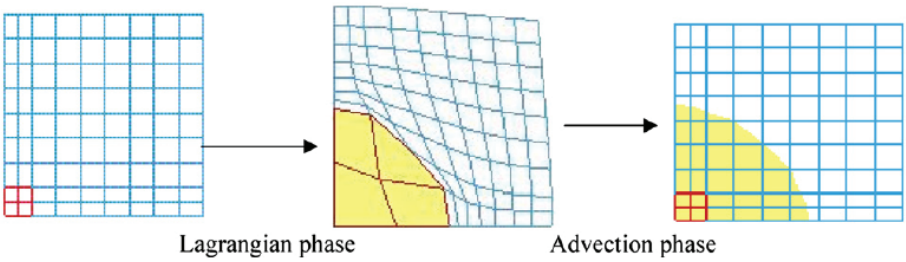

Figure 1: Lagrangian and Advection phases in one step

In the ALE description, an arbitrary referential coordinate is introduced in addition to the Lagrangian and Eulerian coordinates. The material derivative with respect to the reference coordinate can be described in Eq. 1. Thus substituting the relationship between material time derivative and the reference configuration time derivative leads to the ALE equations,

$$\frac{\partial f(X_i,t)}{\partial t} = \frac{\partial f(x_i,t)}{\partial t} + w_i \frac{\partial f(x_i,t)}{\partial x_i} \tag{1}$$

Where X_i is the Lagrangian coordinate, x_i the Eulerian coordinate, w_i is the relative velocity. Let denote by v the velocity of the material and by u the velocity of the mesh. In order to simplify the equations we introduce the relative velocity$w = v - u$. Thus the governing equations for the ALE formulation are given by the following conservation equations:

(i) *Mass equation.*

$$\frac{\partial \rho}{\partial t} = -\rho \frac{\partial v_i}{\partial x_i} - w_i \frac{\partial \rho}{\partial x_i} \tag{2}$$

(ii) *Momentum equation.*

$$\rho \frac{\partial v_i}{\partial t} = \sigma_{ij,j} + \rho b_i - \rho w_i \frac{\partial v_i}{\partial x_j} \tag{3}$$

σ_{ij} is the stress tensor defined by $\sigma = -P.Id + \tau$, where τ is the shear stress from the constitutive model, and P the pressure. For fluid and explosive gas the pressure is computed through an equation of state defined in chapter.

For the structure, a classical elasto-plastic material model is used, where the shear strength is much higher than the volumetric strain.

(iii) *Energy equation.*

$$\rho \frac{\partial E}{\partial t} = \sigma_{ij} v_{i,j} + \rho b_i v_i - \rho w_j \frac{\partial E}{\partial x_j} \tag{4}$$

Note that the Eulerian equations commonly used in fluid mechanics by the CFD community, are derived by assuming that the velocity of the reference configuration is zero, $u = 0$ and that the relative velocity between the material and the reference configuration is therefore the material velocity, $w = v$. The term in the relative velocity in Eq. 3 and Eq. 4 is usually referred to as the advective term, and accounts for the transport of the material past the mesh. It is the additional term in the equations that makes solving the ALE equations much more difficult numerically than the Lagrangian equations, where the relative velocity is zero.

There are two ways to implement the ALE equations, and they correspond to the two approaches taken in implementing the Eulerian viewpoint in fluid mechanics. The first way solves the fully coupled equations for computational fluid mechanics; this approach used by different authors can handle only a single material in an element as described for example in Ozdemir, Souli and Fahjan (2010). The alternative approach is referred to as an operator split in the literature, where the calculation, for each time step is divided into two phases. First a Lagrangian phase is performed, in which the mesh moves with the material, in this phase the changes in velocity and internal energy due to the internal and external forces are calculated. The equilibrium equations are:

$$\rho \frac{\partial v_i}{\partial t} = \sigma_{ij,j} + \rho b_i \ , \tag{5}$$

$$\rho \frac{\partial E}{\partial t} = \sigma_{ij} v_{i,j} + \rho b_i v_i \ . \tag{6}$$

In the Lagrangian phase, mass is automatically conserved, since no material flows across element boundaries.

In the second phase, the advection phase, transport of mass, energy and momentum across element boundaries are computed; this may be thought of as remapping the displaced mesh at the Lagrangian phase back to its original for Eulerian formulation or arbitrary position for ALE formulation using smoothing algorithms. From a discretization point of view of Eq. 5 and Eq. 6, one point integration is used for efficiency and to eliminate locking as it is mentioned by Benson (1992). The zero energy modes are controlled with an hourglass viscosity, see Belytschko (2000). A shock viscosity with linear and quadratic terms derived by Von Neumann and Richtmeyer (1950), is used to resolve the shock wave. The resolution is advanced in time with the central difference method, which provides a second order accuracy for time integration.

For each node, the velocity and displacement are updated as follows:

$$\begin{aligned} u^{n+1/2} &= u^{n-1/2} + \Delta t . M^{-1} . (F_{exl} + F_{int}) \\ x^{n+1} &= x^{n-1} + \Delta t u^{n+1/2} \end{aligned} \tag{7}$$

Where F_{int} is the internal vector force and F_{ext} the external vector force associated with body forces, coupling forces, and pressure boundary conditions, M is a diagonal lumped mass matrix. For each element of the mesh, the internal force is computed as follows:

$$F_{int} = \sum_{k=1}^{Nelem} - \int_k B^t . \sigma . dv \tag{8}$$

Where B is the gradient matrix and *Nelem* is the number of elements.

The time step size Δt, is limited by the Courant stability condition (see Benson (1992)), which may be expressed as:

$$\Delta t \leq \frac{l}{c} \tag{9}$$

Where l is the characteristic length of the element, and c the speed of sound through the material in the element. For a solid material, the speed of sound is defined as:

$$c = \sqrt{\frac{K}{\rho}} \tag{10}$$

Where ρ is the material density, K is the module of compressibility.

3 SPH Formulation

3.1 Standard SPH Formulation

The SPH method developed originally for solving astrophysics problem has been extended to solid mechanics by Libersky, Petschek, Carney, Hipp and Allahdadi (1993) to model problems involving large deformation including high velocity impact. SPH method provides many advantages in modeling severe deformation as compared to classical FEM formulation which suffers from high mesh distortion. The method was first introduced by Lucy (1977) and Gingold and Monaghan (1977) for gas dynamic problems and for problems where the main concern is a set of discrete physical particles than the continuum media. The method was extended to solve high velocity impact in solid mechanics, CFD applications governed by Navier-Stokes equations and fluid structure interaction problems. It is well known from previous papers, see Vignjevic, Reveles and Campbell (2006), that SPH method suffers from lack of consistency, that can lead to poor accuracy of motion approximation. Unlike Finite Element, interpolation in SPH method cannot reproduce constant and linear functions.

A detailed overview of the SPH method is developed by Liu M.B. and Liu G.R.(2010), where the two steps for representing of function f, an integral interpolation and a kernel approximation are given by:

$$u(x_i) = \int u(y).\delta(x_i - y)dy \tag{11}$$

Where the Dirac function satisfies:

$$\begin{aligned} &\delta(x_i - y) = 1, \text{ if } x_i = y \\ &\delta(x_i - y) = 0, \text{ if } x_i \neq y \end{aligned} \tag{12}$$

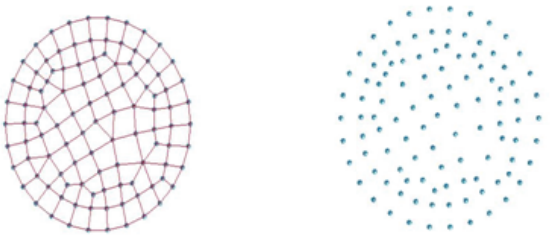

Figure 2: FEM model, mesh and nodes (left) and SPH model, particles (right)

The approximation of the integral function Eq. 11 is based on the kernel approximation W, that approximates the Dirac function based on the smoothing length h.

$$W(d,h) = \frac{1}{h^{\alpha}}.\theta\left(\frac{d}{h}\right) \quad , \tag{13}$$

that represents support domain of the kernel function, see Fig. 3.

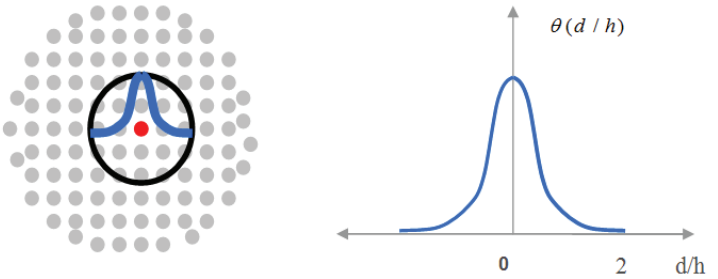

Figure 3: Kernel Function and its support domain for a 2D function

So that Eq 11 becomes,

$$< u(x_i) >= \int u(y).W\left(\|x-y\|,h\right)dy \tag{14}$$

Taking in consideration de support domain of the kernel function, the SPH approximation of a particle x_i is obtained discretizing the integral into a sum over the particles that are within the kernel support domain as it is shown in Fig. 3.

$$u_{sph}(x_i) = \sum_{j\in D_i} \omega_j.u_j.W\left(\left\|x_i - x_j\right\|,h\right), \tag{15}$$

Where the weight $\omega_j = \frac{m_j}{\rho_j}$ is the volume of the particle.

Integrating by part Eq. 14 and considering the properties of the SPH interpolation and that$\nabla(u) = u.\nabla(1) - 1.\nabla(u)$, the SPH approximation for the gradient operator of a function is given by,

$$\nabla u_{sph}(x_i) = \sum_{j\in D_i} \omega_j.(u_i - u_j).\nabla W\left(\left\|x_i - x_j\right\|, h\right), \tag{16}$$

Considering that $\frac{\nabla(P)}{\rho} = \frac{P}{\rho^2}\nabla(\rho) + \nabla\left(\frac{P}{\rho}\right)$, applying the SPH interpolation on Navier-Stokes equations, one can derive a symmetric SPH formulation for Navier-Stokes equations such that the principle of action and reaction is respected and that the accuracy is improved. Finally, we have the following discretized set of equations :

(i) *Mass equation.*

$$\frac{D\rho_i}{Dt} = \rho_i \sum_{j\in D_i} \omega_j.\left(v_i^\beta - v_j^\beta\right).\frac{\partial W\left(\left\|x_i - x_j\right\|, h\right)}{\partial x_i^\beta} \tag{17}$$

(ii) *Momentum equation.*

$$\frac{Dv_i^\alpha}{Dt} = \sum_{j\in D_i} m_j.\left(\frac{\sigma_i^{\alpha\beta}}{\rho_i^2} + \frac{\sigma_j^{\alpha\beta}}{\rho_j^2}\right).\frac{\partial W\left(\left\|x_i - x_j\right\|, h\right)}{\partial x_i^\beta} + f_{ext} \tag{18}$$

(iii) *Energy equation.*

$$\frac{De_i}{Dt} = \frac{1}{2}\sum_{j\in D_i} m_j.\left(\frac{P_i}{\rho_i^2} + \frac{P_j}{\rho_j^2}\right).\left(v_i^\beta - v_j^\beta\right)\frac{\partial W\left(\left\|x_i - x_j\right\|, h\right)}{\partial x_i^\beta} + \frac{\mu_i}{\rho_i}\varepsilon_i^{\alpha\beta}\varepsilon_i^{\alpha\beta} \tag{19}$$

For constant and linear function, The standard SPH interpolation is not exact:

$$\text{For } u(x_i) = 1,\ \sum_{j\in D_i} \omega_j..W\left(\left\|x_i - x_j\right\|, h\right) \neq 1 \tag{20}$$

$$\text{For } u(x_i) = x_i,\ \sum_{j\in D_i} \omega_j.x_j.W\left(\left\|x_i - x_j\right\|, h\right) \neq x_i \tag{21}$$

It is well know from previous studies [see Villa (1999,2005) and Oger(2006)] that Eq.20 and Eq.21 are exact only if the condition $\frac{\Delta x}{h} \to 0$, as it is shown in Fig.4, which is not numerically possible and it is a severe limitation to the method because the consistency and the convergence of the method are not guaranteed and thus it affects the accuracy of the standard SPH method. In order to improve the standard SPH solution a renormalization technique has been introduced.

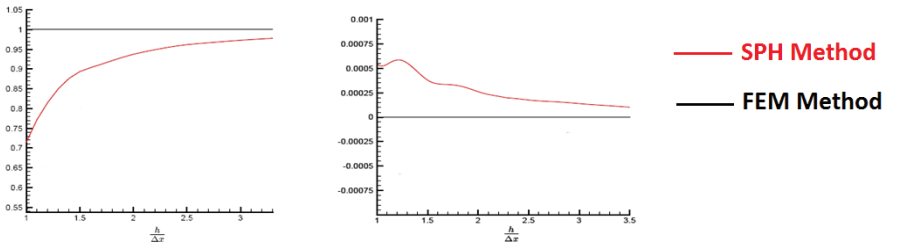

Figure 4: Linear representation of o a constant function (left) and its relative error (right)

3.2 Renormalized SPH Formulation

The derivative of constant functions can be represented exactly (far from a boundary) by the standard SPH even for disordered particles using the symmetrical approximation for the gradient operator Eq.16 but it still not the case for linear functions. In order to improve the accuracy of the SPH Method a renormalized operator has been introduced by Randles and Libersky(1996). The employed technique enforces the exact representation of constant and linear functions and its derivate by introduction a renormalization matrix B correcting the differential gradient operator in Eq.16 such that for$u(x) = a + b.x$, we have for a particle "i":

$$\nabla u_{sph}(x_i) = b : \sum_{j \in D_i} \omega_j . (x_i - x_j) . \nabla W \left(\left\| x_i - x_j \right\|, h \right) : B_i = b : Id \tag{22}$$

$$\Rightarrow \sum_{j \in D_i} \omega_j . (x_i - x_j) . \nabla W \left(\left\| x_i - x_j \right\|, h \right) : B_i = Id$$

Finally we identify the correction matrix $B_i$for a particle "i":

$$B_i = E_i^{-1},$$

where

$$E_i = \sum_{j \in D_i} \omega_j . (x_i - x_j) . \nabla W \left(\left\| x_i - x_j \right\|, h \right) \tag{23}$$

For a 2D problem, let $x_i = (a_i, b_i)$ and $r_{ij=} \left\| x_i - x_j \right\|$ then we have :

$$E_i = \begin{bmatrix} -\sum_{j \in D_i} \omega_j . \frac{dW}{dr} \frac{(a_j - a_i)^2}{r_{ij}} & -\sum_{j \in D_i} \omega_j . \frac{dW}{dr} \frac{(a_j - a_i)(b_j - b_i)}{r_{ij}} \\ -\sum_{j \in D_i} \omega_j . \frac{dW}{dr} \frac{(a_j - a_i)(b_j - b_i)}{r_{ij}} & -\sum_{j \in D_i} \omega_j . \frac{dW}{dr} \frac{(b_j - b_i)^2}{r_{ij}} \end{bmatrix} \tag{24}$$

In addition to the improvement of the consistency of the method, Lanson (2003) and Vila (2005) have also shown that the renormalization technique relax the convergence criterion $\frac{\Delta x}{h} \to 0$ to be $\frac{\Delta x}{h} \to o(1)$ improving the global convergence of the method.

4 Constitutive models and equation of states for explosive and water materials

In High explosive process, a rapid chemical reaction is involved, which converts the material into high pressure gas. From a constitutive material point of view, the gas is assumed inviscid with zero shear, and the pressure is computed through JWL equation of state (Jones-Wilkins-Lee), a specific equation of state, commonly used for explosive material. There have been many equations of state proposed for gaseous products of detonation, from simple theoretically to empirically based equations of state with many adjustable parameters, see Hallquist (1998). The explosive was modelled with 8-nodes elements. The equation of state determines the relation between blast pressure, change of volume and internal energy. The JWL equation of state was used in the following form :

$$p = A\left(1-\frac{\omega}{R_1 V}\right)\exp\left(-R_1 V\right)+B\left(1-\frac{\omega}{R_2\omega}\right)\exp\left(-R_2 V\right)+\frac{\omega}{V}E \tag{25}$$

In Equation (25) p is the pressure, V is the relative volume defined by $V=\frac{v}{v_0}$.

Where v and v_0 are the current and initial element volume respectively, while A, B, C, R_1,R_2 and ω are material constants. These performance properties are based on the cylinder expansion test in controlled conditions.

At the beginning of the computations V=1.0 and E is the initial energy per unit volume.

The first term of JWL equation, known as high pressure term, dominates first for V close to one. The second term is influential in the JWL pressure for V close to two. Observe that in the expanded state, the relative volume is sufficiently important so that the exponential terms vanish, and JWL equation of state takes the form of an ideal gas equation of state:

$$P = \omega\frac{E}{V} \tag{26}$$

The temperature T can be computer using internal energy:

$$E = C_v.T \tag{27}$$

Where C_v is the average heat capacity. The heat capacity is held constant throughout the calculation.

The JWL equation of state is a macroscopic description of the high explosive detonation, it does not describe chemical reaction between different species of the material, which is a complex phenomena of the explosive burn. The macroscopic description through the JWL equation of state can be used to generate pressure wave

outside the explosive, once all explosive has burned. For a microscopic description of explosive detonation, molecular dynamic theory can be used, as described in detail in Benazzouz and Zaoui (2012).

After detonation, a pressure wave is propagating in a water material governed by the constitutive fluid material model as shown,

$$\sigma = -P.Id + \tau, \text{ where } \tau = 2\mu \dot{\varepsilon} \tag{28}$$

Where μ and $\dot{\varepsilon}$ respectively denote the dynamic viscosity and the strain in rate form. The pressure term is calculated using the Mïe-Gruneïsen equation of state given by:

For compressed material :

$$P = \frac{\rho_0 C^2 \mu \left[1 + \left(1 - \frac{\gamma_0}{2}\right)\mu - \frac{a}{2}\mu^2\right]}{\left[1 - (S-1)\mu\right]^2} + (\gamma_0 + a)\mu E \tag{29a}$$

For expanded material :

$$P = \rho_0 C^2 \mu + (\gamma_0 + a)\mu E \tag{29b}$$

Where P, ρ_0, C and γ_0 are respectively the pressure, the nominal density, the speed of sound and the specific relative volume. γ_0 is the gruneïsen parameter, a is a first order correction to the energy E and S is unitless coefficient of the slope of the Hugoniot shock $u_s - u_p$ curve given by Narsh (1980), where u_s and u_p are respectively the shock and the particle velocities.

Parameters for the explosive material are given in Tab.1 and Tab.2. For the water material are given in Tab.3 and Tab.4.

Table 1: Material model parameters for Explosive

Density (g.cm-3)	Detonation Velocity	Chapman-Jouget Pressure
1.7	0.753	0.255

Table 2: JWL equation of state parameters for Explosive

A	B	R1	R2	ω	E0	$V_0 = \frac{1}{1+\mu}$
5.4094	0.0937260	4.5	1.1	0.35	0.08	0.0

Table 3: Material model parameters Water

Density (g.cm-3)	Cut-off Pressure(Pa)	Dynamic Viscosity(Pa.ms)
1.0	-1.0E-6	0.0

Table 4: Mïe-Gruneïsen equation of state parameters for Water

C (cm.ms-1)	S1	S2	S3	γ_0	a	E0	$V_0 = \frac{1}{1+\mu}$
0.1484	1.979	0.0	0.0	0.11	3.0	0.0	0.0

5 Numerical Simulations

5.1 ALE and SPH Models

In this example, we consider a simple structure in water subjected to blast loading generated though detonation of explosive material. The FEM Structure and ALE Fluid are modelled using eight nodes solid elements, while the SPH elements are generated at the center of the ALE elements. A sketch at Fig.5 illustrates the problem.

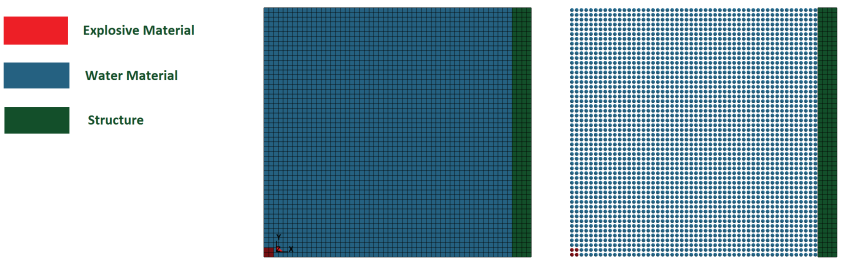

Figure 5: Sketch of the ALE-FEM model (left) and the SPH-FEM model (right)

The fluid structure interaction is modelled for both ALE-FEM and SPH-FEM problems using kinematics type contact algorithm at the fluid structure interface. The kinematic constraints method is used where constraints are imposed on displacement and velocity of the contact interface, as well as impenetrability condition, as described Belytschko and Neal (1989). In addition, a smoothing algorithm is used with the ALE formulation, constraining the nodes to move uniformly along straight lines, to overcome high mesh distortion problems preserving mesh integrity.

Slip boundary conditions are applied to the ALE elements at the top, left and bottom boundaries, whereas the structure is fixed at the top and constrained to move in the X-direction at the bottom.

Definition of proper boundary conditions for SPH formulation is a challenge in the SPH theory. Several techniques has been developed in order to enhance the desired conditions, to stop particle from penetrating solid boundaries and also to complete the kernel function which is truncated by the physical domain for a particle close to the boundary. Among the different techniques, the ghost particle method [see Oger (2006); Colagrossi and Landrini(2003); Doring(2006)] is known to be robust and accurate and is used in the simulations. When a particle is close to the boundary, it is symmetrised across the boundary with the same density, pressure and temperature as its real particle such that mathematical consistency is restored. The ghost particles velocity is adjusted such that slip or stick boundary condition is applied.

In order to treat problem involving discontinuities in the flow variables such as shock waves, an additional dissipative term is added as an artificial pressure term. This artificial viscosity should be acting in the shock layer and should be neglected outside. In this simulation a pseudo-artificial pressure term π_{ij} derived by Monoghan and Gingold (1983) is used. This term is based on the classical Von Neumann and Richtmeyer (1950) artificial viscosity and is readapted to the SPH formulation as follow,

$$\begin{aligned} &\pi_{ij} = \beta\mu_{ij}^2 - \alpha\mu_{ij}c_{ij}^{,} \qquad \text{if } v_{ij}.r_{ij} < 0 \text{ (In the shock layer)} \\ &\pi_{ij} = 0, \qquad\qquad\qquad\quad \text{elsewhere (Outside the shock layer)} \end{aligned} \tag{30}$$

Where $\mu_{ij} = \frac{v_{ij}.r_{ij}}{r_{ij}^2+\varepsilon h_{ij}^2}$, $\rho_{ij} = \frac{(\rho_i+\rho_j)}{2}$ and $c_{ij} = \frac{(c_i+c_j)}{2}$ are respectively the average density and speed of sound, $\varepsilon$is a small perturbation that is added to avoid singularities, finally α and β are respectively the linear and quadratic coefficient.

5.2 Results Comparison and Mesh sensitivity analysis for SPH Method

For this problem ALE multi-material and SPH formulation are used to solve the problem up to physical termination time. As mentioned in the introduction, experimental tests for explosive detonation in fluid and the impact on surrounding structures, are costly to perform. The ALE formulation will be considered as reference solution to validate the SPH formulation since it has been validated against experiments in many applications involving explosions, blast impact and shock waves [see Leblanc and Shukla (2010) or Barras, Souli, Aquelet and Cuty (2012)]. In order to compare ALE and SPH formulations and to check the limits of the SPH formulation solving fluid structure interaction problems, two simulations were performed. A first one, using the same number of elements for both ALE and SPH

methods, such that the space step *dx* separating two particles in the SPH case or the length of an element in the ALE case is the same. A second one, refining the SPH model by two in both direction in order to improve the accuracy of the simulation and to see how the SPH solution behave compared to the ALE one. In both simulations SPH particles are generated at the center of the ALE elements as it is shown in Fig.6.

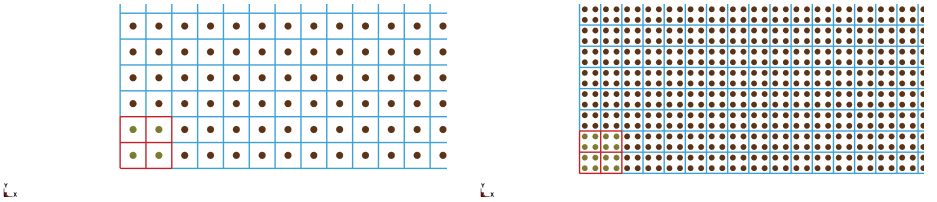

Figure 6: SPH particles generation for the non-refined simulation (left) and the refined simulation (right)

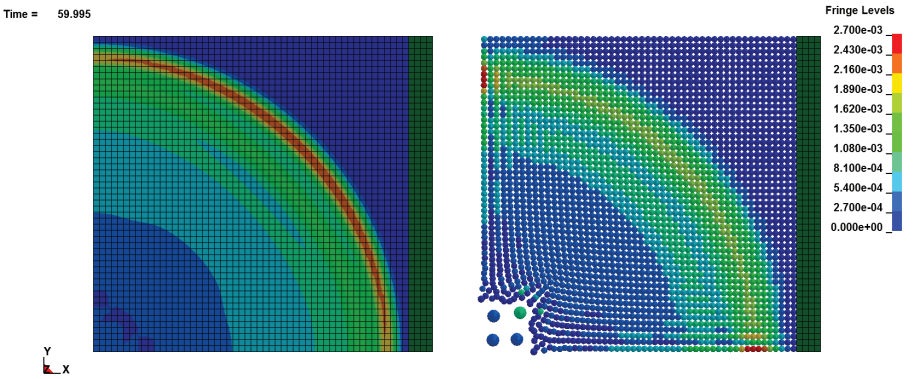

Figure 7: Pressure contour for ALE and non refined SPH models at time t = 60 ms.

To illustrate pressure wave propagation through water material, Fig.7 shows the pressure fringe at time t=60 microseconds from both ALE and non-refined SPH simulations. At this time of the simulation, the structure is not deformed, since the shock wave did not reach the structure yet, and it can be seen that the SPH formulation represents well qualitatively the physics as the shock front and the expansion waves has the same shape in both ALE and non-refined SPH solutions.

In order to compare quantitatively the solutions, the structure is examined where the X-displacement and the X-velocity time curve of a node on the structure are

plotted in Fig.8 and Fig.9 and the Von Mises Stress time curve of an FEM element on the structure is plotted in Fig.10 for both ALE and non-refined SPH formulations up to time t=130 milliseconds. If both ALE and SPH curves have the same shape, they are not fitting which shows the limitation of the method presented in section 3 as a consequence of the convergence criterion be $\frac{\Delta x}{h} \to o(1)$.

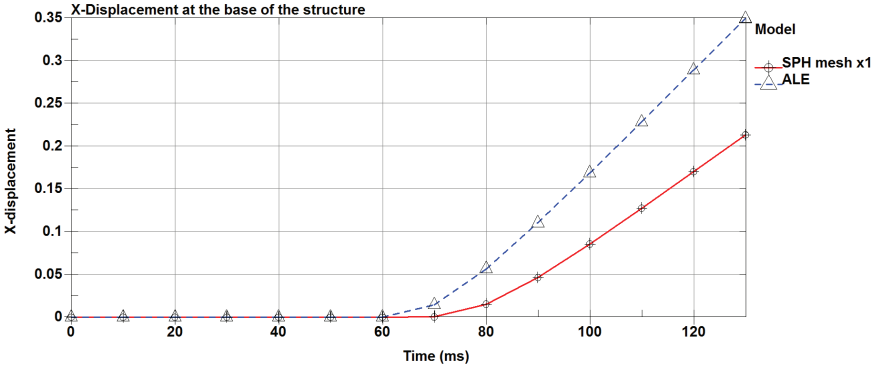

Figure 8: X-displacement of the structure at its base for ALE model and non-refined SPH model

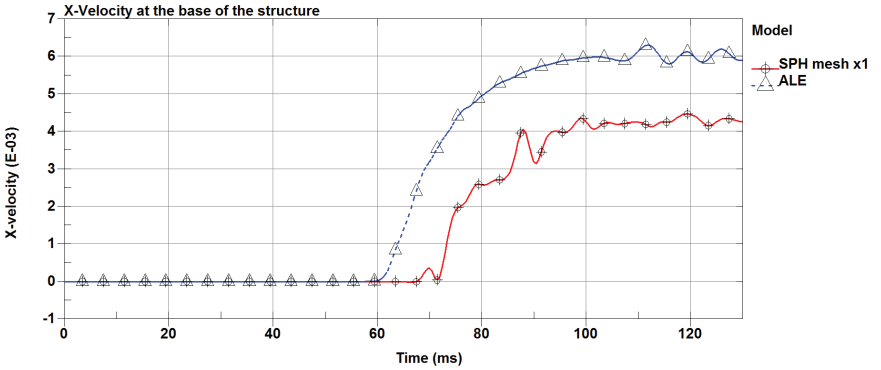

Figure 9: X-Velocity of the structure at its base for ALE model) and non-refined SPH models.

For the refined SPH model, Fig. 11 the pressure fringe is plotted at time t=60 ms and for the refined SPH model and Fig. 12 shows the expansion of the explosive material in the water. and it can be seen that the refined solution is more accurate as the expansion wave. It shows good correlation between the two results and the

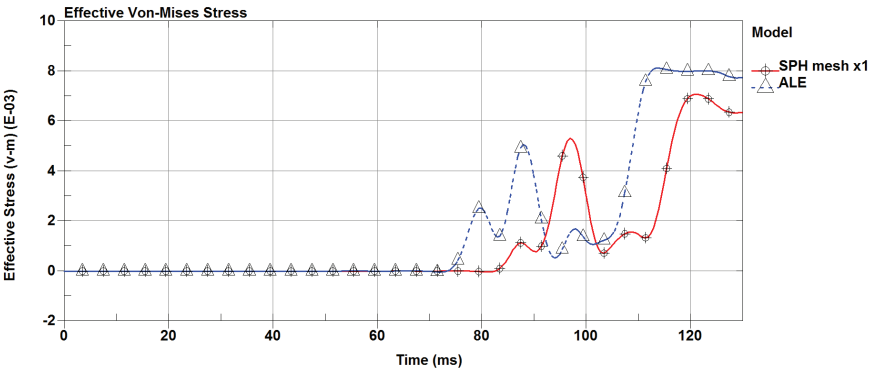

Figure 10: Von Mises stress of the structure at the middle for ALE and non-refined SPH models.

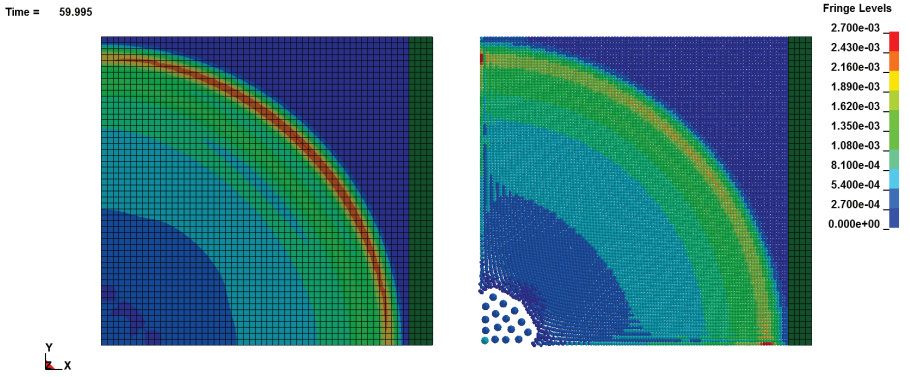

Figure 11: Pressure contour for ALE model and refined SPH models at time t = 60 ms.

ability of the SPH method to handle naturally complex flows involving multiple materials due to its pure langrangian nature. In the case of ALE formulation, it is needed to add to the mixture theory an interface tracking algorithm such as Volume Of Fluid (VOF) method or Level Set method.

In Fig.13, Fig.14, Fig.15 and Fig.16 show good correlation between the two results and that the accuracy of the method has improved refining the SPH model and that compared to ALE approach the SPH methods needs more elements, in particular in this example two times more elements in each direction.

In this work, we have presented the application of SPH and ALE approaches for simulating blast wave propagation in water. Comparisons with experimental re-

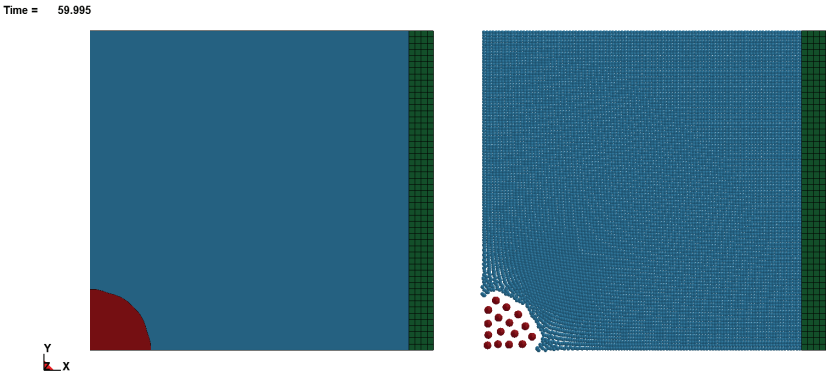

Figure 12: Explosive expansion for ALE and refined SPH models at time t = 60 ms.

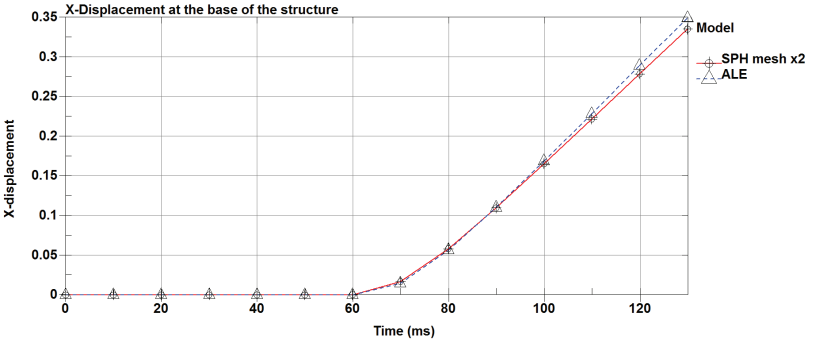

Figure 13: X-displacement of the structure at its base for ALE refined SPH models.

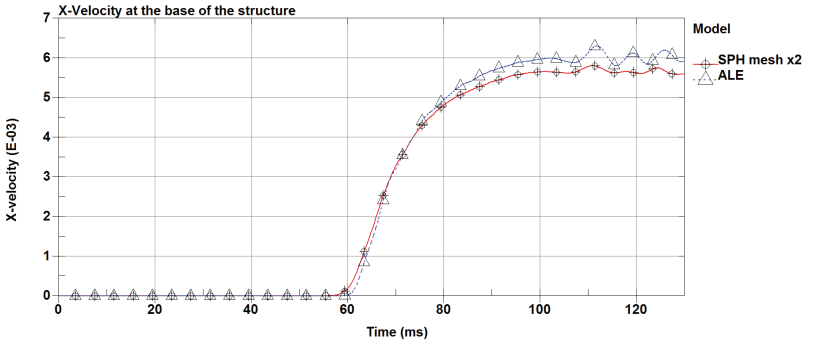

Figure 14: X-Velocity of the structure at its base for ALE and refined SPH models.

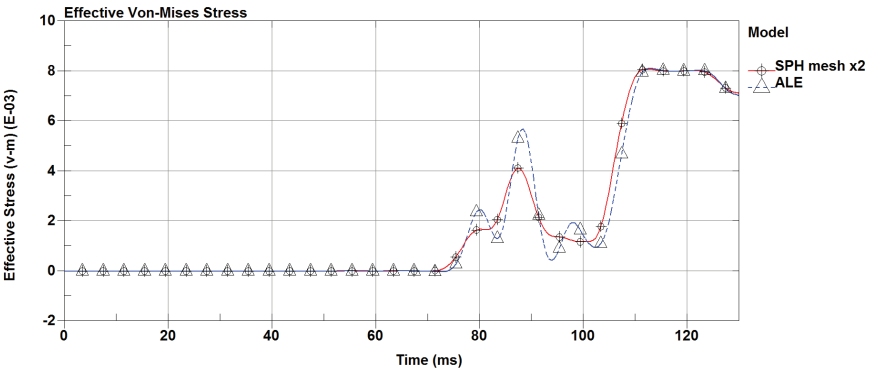

Figure 15: Von Mises stress of the structure at the middle for ALE and refined SPH models.

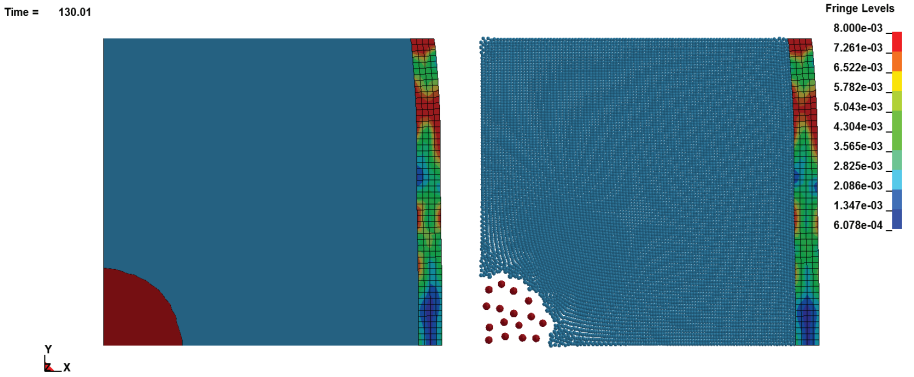

Figure 16: Von Mises stress on the FEM structure subjected to the shock wave in the ALE and refined SPH models at time t = 130 ms.

sults from literature and CONWEP predictions were made in order to validate the numerical model. Several parametric studies were conducted.

Once simulations are validated by test results, it can be used as design tool for the improvement of the system structure involved.

6 Conclusion

In this paper we present ALE and SPH methods as well as their limitations for specific problems. Underwater explosion is commonly solved using ALE formulation, in defence industry; some of these problems are solved using SPH method. For the last decade, SPH methods are gaining in accuracy numerical stability, and the use

of SPH method is becoming more common in industry for solving fluid structure coupling problems. For instance, in aerospace, where bird impacts on aircraft are very common and cause significant safety threats to commercial and military aircraft. According to FAA (Federal American Aviation) regulations, aircraft should be able to land safely, see Souli and Gabrys (2012). For decades engineers in aerospace industry were using ALE method to simulate bird impact on aircrafts, where a viscous hydrodynamic material is used for the bird. These applications require a large ALE domain for the coupling between the bird material and the surrounding structure, mainly when the bird is spread all over the space. According to technical reports from engineers in aerospace, ALE formulation is more CPU time consuming and requires more memory allocation that SPH method. In this paper, first we describe both ALE and SPH methods, and we compare numerical results between the two methods using similar mesh size, each ALE element is replaced by an SPH particle at the element center. Using a simple fluid structure interaction problem, it has been observed that using same mesh size for both methods, numerical results, displacement, velocity and Von Mises stress on the structure, are underestimated with SPH method. When refining the SPH particles, where each ALE element is replaced by 4 SPH particles in two dimensional and 8 particles in three dimensions, numerical results form SPH method are in good correlation with those from ALE simulation; in terms of displacement, velocity and Von Mises stress on the structure. Since the ultimate objective is the design of structure resisting to load blast, numerical simulations from ALE and SPH methods can be included in shape design optimization with shape optimal design techniques, see Souli and Zolesio (1993), and material optimisation, see Erchiqui, Souli and Ben Yedder (2007). Once simulations are validated by test results, they can be used as design tool for the improvement of the system structure being involved.

References

Aquelet, N.; Souli, M.; Olovson, L. (2005): Euler Lagrange coupling with damping effects: Application to slamming problems. *Computer Methods in Applied Mechanics and Engineering*, vol. 195, pp. 110-132.

Barras, G.; Souli, M.; Aquelet, N.; Cuty, N. (2012) : Numerical simulation of underwater explosions using ALE method. The pulsating bubble phenomena. *Ocean Engineering,* vol. 41, pp. 53-66.

Belytschko, T.; Neal MO. (1989) : Contact-impact by the pinball algorithm with penalty, projection, and Lagrangian methods. *Proceedings of the symposium on computational techniques for impact, penetration, and perforation of solids AMD,* vol.103, New York, NY: ASME, pp. 97–140.

Belytschko, T.; Liu, W.K.; B. Moran. (2000) : *Nonlinear Finite Elements for Continua and Structure. Wiley.*

Benson, D. J. (1992) : Computational Methods in Lagrangian and Eulerian Hydrocodes. *Computer Method Applied Mech. and Eng,* vol. 99, pp. 235-394.

Benazzouz, B. K; Zaoui, A. (2012) :Thermal behavior and super heating temperature of Kaolinite from molecular dynamics. *Applied Clay Science,* vol. 58, pp. 44-51.

Boyer, D.W. (1960) : An experimental study of the explosion generated by a pressurized sphere. *Journal of Fluid Mechanics,* vol. 9, pp. 401–429.

Colagrossi, A.; Landrini, M. (2003) : Numerical simulation of interfacial flows by smoothed particle hydrodynamics. *Journal of Computational Physics,* vol. 191, pp. 448.

Doring, M. (2006) : Développement d'une méthode SPH pour les applications à surface libre en hydrodynamique. *PhD thesis, Ecole Centrale de Nantes, France.*

Erchiqui, F.; Souli, M.; Ben Yedder, R. (2007): Non isothermal finite-element analysis of thermoforming of polyethylene terephthalate sheet: Incomplete effect of the forming stage. *Polymer Engineering and Science,* vol. 47 , pp. 2129-2144.

Gingold, R. A.; Monaghan, J. J. (1977) :Smoothed particle hydrodynamics: theory and applications to non-spherical stars. *Mon. Not.R. Astr. Soc,* vol. 181, pp. 375–389.

Hallquist, J. O. (1998) : *LS-DYNA THEORY MANUEL. Livermore Software Technology Corporation.*

Kingery, C.; Bulmarsh, G. (1984) : Airblast Parameters from TNT spherical air burst and hemispherical surface burst. *ARBRL-TR-02555, U.S. Army Ballistic*

Lanson, N. (2003) : Etude des méthodes particulaires renormalisées. Applications aux problèmes de dynamique rapide. *PhD Thesis, Université Toulouse 3 INSA*

Leblanc, J.; Shukla, A. (2010) : Dynamic response and damage evolution in composite materials subjected to underwater explosive loading: An experimental and computational study. *Composite Structures,* vol. 92, pp. 2421-2430.

Libersky, L. D.; Petschek, A. G.; Carney, T. C.; Hipp, J. R., Allahdadi, F. A. (1993) : High Strain Lagrangian Hydrodynamics: A Three-Dimensional SPH CODE for Dynamic Material Response. *Journal of Computational Physics,* vol. 109, pp. 67-75.

Lucy, L. B. (1977): A numerical approach to the testing of fission hypothesis. *Astronom. J.* vol. 82, pp. 1013–1024.

Liu, M. B.; Liu, G. R. (2010) : Smoothed Particle Hydrodynamics (SPH): an

Overview and Recent Developments. *Arch Comput Methods Eng,* vol. 17, pp. 25–76.

Monaghan, J. J.; Gingold, R. A. (1983) : Shock Simulation by particle method SPH. *Journal of Computational Physics,* vol. 52, pp. 374-389.

Narsh, S. P. (1980) : *LASL Shock Hugoniot Data.* University of California Press.

Oger, G. (2006) : Aspects théoriques de la méthode SPH et applications a l'hydrodynamique a surface.

PhD Thesis, Ecole Centrale de Nantes

Ozdemir, Z.; Souli, M.; Fahjan Y.M. (2010) : Application of nonlinear fluid–structure interaction methods to seismic analysis of anchored and unanchored tanks. *Engineering Structures,* vol. 32, pp. 409-423.

Randles, P. W.; Libersky, L. D. (1996) : Smoothed Particle Hydrodynamics: Some recent improvements and applications. *Comput. Methods Appl. Mech. Engrg,* vol. 139, pp. 375-408.

Souli, M.; Zolesio, J. P. (1993): Shape Derivative of Discretized Problems. *Computer Methods in Applied Mechanics and Engineering,* vol. 108, pp. 187–199.

Souli, M.; Erchiqui, F. (2011) : Experimental and Numerical investigation of hyperelastic membrane inflation using fluid structure coupling. *Computer Modeling in Engineering & Sciences,* vol. 77, pp. 183-200.

Souli, M.; Gabrys, J. (2012) : Fluid Structure Interaction for Bird Impact Problem: Experimental and Numerical Investigation. *CMES,* vol. 2137, no. 1, pp. 1-16.

Vignjevic, R; Reveles, J.; Campbell, J. (2006): SPH in a Total Lagrangian Formalism. *Computer Modelling in Engineering and Science,* vol. 14, pp. 181-198.

Vila, J. (1999) : On particle weighted method and smoothed particle hydrodynamics. *Mathematical Models and Method in Applied Science,* vol. 9, pp. 161-209.

Vila, J. (2005): SPH renormalized hybrid methods for conservation laws: applications to free surface flows.Mesh free Methods for Partial Differential Equations II. *Vol.43 of Lecture Notes in Computational Science and Engineering. Springer*

Von Neumann, J.; Richtmeyer, R. D. (1950): A method for the numerical calculation of hydrodynamical shocks. *Journal of Applied Physics,* vol. 21, pp. 232.